

complexes. There seems to be angular strain in the cage caps, whereas the en fragments exhibit angles close to the tetrahedral value. This is consistent with the ease of deprotonation and the observed specificity of amine dehydrogenation in Ru(sar)³⁺.

Acknowledgment. P.B. thanks Prof. A. Ludi (Bern, Switzerland) for financial support. We gratefully acknowledge financial help by the "Schweizerischer Nationalfonds zur Förderung der

wissenschaftlichen Forschung". We thank Prof. G. B. Jameson for a copy of his twin refinement program.¹⁹

Supplementary Material Available: Listings of calculated hydrogen positional parameters, anisotropic displacement parameters, crystal data, intensity collection, and refinement parameters, and hydrogen bond distances and angles (7 pages); listings of observed and calculated structure factors (18 pages). Ordering information is given on any current masthead page.

Contribution from the Departments of Chemistry, The University of Trondheim, N-7055 Dragvoll, Trondheim, Norway, and The University of Reading, Whiteknights, Reading RG6 2AD, U.K.

Gas-Phase Electron Diffraction Study of Bis(dimethyldithiocarbamato)copper(II), [Cu(S₂CNMe₂)₂], and Bis(dimethyldithiocarbamato)zinc(II), [Zn(S₂CNMe₂)₂]

Kolbjørn Hagen,^{1a} Catherine J. Holwill,^{1b} and David A. Rice*^{1b}

Received January 31, 1989

The molecular structures of [Cu(S₂CNMe₂)₂] and [Zn(S₂CNMe₂)₂] have been studied by gas-phase electron diffraction. Both compounds are monomeric in the gas phase with the metal atoms being bound to two chelating [S₂CNMe₂] groups ($r_g(\text{Cu-S}) = 2.284$ (9) Å; $r_g(\text{Zn-S}) = 2.348$ (8) Å). The major difference between the two structures is in the geometry of the MS₂ fragments, that of the copper compounds being pseudo square planar (D_{2h}) while that of the zinc compound is pseudotetrahedral (D_{2d}). The reason for the difference is attributed to the availability in the copper(II) compound of crystal field stabilization energy that is greater than the repulsive energy of the steric interactions imposed by the metal adopting a coordination sphere of D_{2h} symmetry. Selected bond lengths and angles in the [S₂CNMe₂] groups are as follows (the data for the copper compound are quoted first with those for the zinc species being in brackets): $r_g(\text{C-S}) = 1.716$ (10) Å [1.727 (10) Å]; $r_g(\text{C=N}) = 1.334$ (18) Å [1.351 (17) Å]; $r_g(\text{C-N}) = 1.476$ (18) Å [1.479 (17) Å]; $\angle \text{S-M-S}$ (chelate angle) = 78.78 (69)° [79.68 (59)°]; $\angle \text{C=N-C} = 124.9$ (1.3)° [122.5 (1.2)°].

Introduction

The geometry of the coordination sphere exhibited by a metal in one of its complexes can often be predicted from a consideration of simple crystal field theory, a knowledge of the d^n configuration of the metal, and the nature of the ligands in the compound. For example nickel(II), which is d^8 , is expected to form square-planar complexes with ligands high in the spectrochemical series and tetrahedral ones with ligands low in the series. Thus, [NiCl₄]²⁻ was predicted to be tetrahedral and [Ni(CN)₄]²⁻ square planar. Confirmation of the predictions was achieved through single-crystal X-ray diffraction studies. However, in the solid state, packing forces may influence the coordination geometry exhibited by a metal ion; thus, the agreement between prediction and the results of single-crystal X-ray diffraction studies may be fortuitous. In the gas phase packing forces are eliminated; thus, the comparison between prediction and the structural results from gas-phase electron diffraction studies provide a valid test for predictions. However, while there have been numerous studies of coordination compounds by single-crystal X-ray diffraction, only a small number have been examined by gas-phase electron diffraction and those that have been studied possess either oxygen or nitrogen in the coordination sphere. Crystal effects are important. For example, with the ligand [MeCOCHCOMe]⁻, which is low in the spectrochemical series, nickel(II) forms [Ni(MeCOCHCOMe)₂], which is trimeric in the solid state with all three metal atoms being six-coordinate,² while in the gas phase it is monomeric with the metal having a planar (pseudo square planar) coordination sphere of four oxygen atoms.³

In view of the paucity of electron diffraction data for coordination compounds and yet the usefulness of such data that do exist, we decided to attempt to extend the range of compounds that have been studied in the gas phase to some simple compounds having sulfur ligands. We now report a study of the structures of bis(dimethyldithiocarbamato)copper(II), [Cu(S₂CNMe₂)₂], and bis(dimethyldithiocarbamato)zinc(II), [Zn(S₂CNMe₂)₂]. The

existence of reports of single-crystal X-ray studies on both compounds^{4,5} influenced the choice of compounds for investigation.

Experimental Section and Analysis of the Structure

Preparation of Bis(dimethyldithiocarbamato)zinc(II), [Zn(S₂CNMe₂)₂], and Bis(dimethyldithiocarbamato)copper(II), [Cu(S₂CNMe₂)₂]. Zinc(II) chloride or copper(II) chloride (0.01 mol) was dissolved in the minimum quantity of ethanol. To this was added a saturated ethanolic solution of sodium dimethyldithiocarbamate (0.02 mol). Immediate precipitation took place, and the compounds were isolated by filtration and washed with ethanol. The samples had metal, carbon, hydrogen, and nitrogen analyses in accord with the formulation [M(S₂CNMe₂)₂] (M = Cu, Zn).

The Reading Apparatus. Electron diffraction data were obtained by using the apparatus built at the University of Reading. Full details of the apparatus have been given elsewhere.⁶

The experimental conditions used to obtain data for [Zn(S₂CNMe₂)₂] and [Cu(S₂CNMe₂)₂] are as follows. Three plates were examined at both long and short camera distances for both compounds, the camera distances being 494.51 and 244.33 mm. The electron wavelength was 0.061 54 Å. The nozzle temperatures were 275 °C for the copper species and 260 °C for the zinc compound. Unfortunately the s range of the usable data was restricted to 3.75–12.00 and 9.00–25.00 Å⁻¹ for the long and short camera distances, respectively. This cutoff for usable data, 12.00 and 25.00 Å⁻¹ for the long and short camera distances, respectively, we believe is caused by sample being deposited upon the plate when high nozzle temperatures are used. This effect has been noted previously.⁶

The experimental data were processed as previously described⁷⁻¹¹ with

* To whom correspondence should be addressed.

- (1) (a) The University of Trondheim. (b) The University of Reading.
- (2) Bullen, J. C.; Mason, R.; Pauling, P. *Inorg. Chem.* **1965**, *4*, 456.
- (3) Shibata, S.; Ohia, M.; Tani, R. *J. Mol. Struct.* **1981**, *73*, 119.
- (4) Einstein, F. W. B.; Field, J. S. *Acta Crystallogr.* **1974**, *B30*, 2928.
- (5) Klug, H. P. *Acta Crystallogr.* **1966**, *21*, 536.
- (6) Holwill, C. J. Ph.D. Thesis, University of Reading, Reading, U.K., 1987.
- (7) Hagen, K.; Hedberg, K. *J. Am. Chem. Soc.* **1973**, *95*, 1003.
- (8) Gundersen, G.; Hedberg, K. *J. Chem. Phys.* **1969**, *51*, 2500.
- (9) Andersen, B.; Seip, H. M.; Strand, T. G.; Stølevik, R. *Acta Chem. Scand.* **1969**, *23*, 3224.
- (10) Hagen, K.; Hobson, R. J.; Holwill, C. J.; Rice, D. A. *Inorg. Chem.* **1986**, *25*, 3659.
- (11) Hedberg, L. *Abstracts of Papers*, 5th Austin Symposium on Gas-Phase Molecular Structure, Austin, TX, March 1974; p 37.

Table I. Final Structural Parameters for $[\text{Cu}(\text{S}_2\text{CNMe}_2)_2]$ and $[\text{Zn}(\text{S}_2\text{CNMe}_2)_2]^a$

param	$[\text{Cu}(\text{S}_2\text{CNMe}_2)_2]$			$[\text{Zn}(\text{S}_2\text{CNMe}_2)_2]$		
	r_g	l_{refined}	l_{calc}	r_g	l_{refined}	l_{calc}
Independent Parameters						
$r(\text{M}-\text{S})$	2.284 (9)	0.092 (9)	0.080	2.348 (8)	0.077 (11)	0.083
$r(\text{C}-\text{S})$	1.716 (10)	0.024 (25)	0.047	1.727 (10)	0.0496	0.049
$r(\text{C}-\text{N}_{\text{av}})$	1.405 (18)	0.080 (44)	0.046	1.415 (17)	0.014 (60)	0.046
$\Delta r(\text{C}-\text{N})^c$	0.142			0.128		
$r(\text{C}-\text{H})$	1.108 (61)	0.100 (59)	0.079	1.102 (43)	0.070 (49)	0.079
$\angle \text{S}_2-\text{M}-\text{S}_3$	78.78 (69)			79.68 (59)		
$\angle \text{N}-\text{C}-\text{H}$	99.2 (6.4)			106.9 (7.9)		
$\angle \text{C}_6-\text{N}_8-\text{C}_{10}$	124.9 (1.3)			122.5 (1.2)		
Φ_1	0.0 ^d			90.0 ^d		
Selected Dependent Parameters						
$\angle \text{S}_2-\text{M}-\text{S}_4$	180.0 (3)			126.1 (4)		
$r(\text{S}_2 \cdots \text{S}_3)^e$	2.904 (22)	0.079 (14)	0.064	3.007 (13)	0.070 (15)	0.063
$r(\text{S}_2 \cdots \text{S}_5)^e$	3.539 (16)	0.154 (14)	0.140	4.184 (13)	0.132 (15)	0.126
$r(\text{S}_2 \cdots \text{S}_4)^e$	4.575 (13)	0.126 (14)	0.114	4.181 (13)	0.128 (15)	0.127
$r(\text{C}_6-\text{N}_8)^f$	1.334 (18)	0.080 (44)	0.046	1.351 (17)	0.035 (60)	0.046
$r(\text{C}_{10}-\text{N}_8)^f$	1.476 (18)	0.087 (44)	0.053	1.479 (17)	0.023 (60)	0.053
$r(\text{M}-\text{C}_6)$	2.690 (21)	0.129 (35)	0.078	2.644 (22)	0.105 (135)	0.081

^a Distances (r_g) and amplitudes (l) in angstroms, and angles (\angle) in degrees. Uncertainties, shown in parentheses, are 2σ and include estimates of systematic errors and correlation in the experimental data. ^b Kept fixed at calculated value. ^c Kept constant in the final refinement. ^d These values were fixed, as from early refinements it was revealed that deviations from 0.0° for $\text{M} = \text{Cu}$ and 90° for $\text{M} = \text{Zn}$ were not statistically significant. ^e Amplitudes for these distances refined as a group. ^f Amplitudes for these distances refined as a group.

scattering factors taken from Ref 12 and 13. Figure 1 contains representations of the molecules together with the atom-numbering scheme that was used. In choices of the models for the two compounds a number of assumptions were made, namely (1) the Me groups have C_{3v} symmetry with the axis coincident with the adjacent N-C bond, (2) within a S_2CNMe_2 group the S_2CNC_2 fragment is planar and has C_{2v} symmetry, (3) the CuS_4 fragment has D_{2h} symmetry while the symmetry of the ZnS_4 moiety is D_{2d} , and (4) for a given molecule all M-S bonds are equivalent. Thus, the model was defined by five bonding distances ($r(\text{C}-\text{H})$, $r(\text{C}_6-\text{N}_8)$, $r(\text{C}_{10}-\text{N}_8)$, $r(\text{C}_6-\text{S}_2)$, and $r(\text{M}-\text{S})$ ($\text{M} = \text{Cu}, \text{Zn}$)) three valence angles ($\angle \text{S}_3-\text{M}-\text{S}_2$, $\angle \text{N}-\text{C}-\text{H}$, and $\angle \text{C}_6-\text{N}_8-\text{C}_{10}$), and the interplanar angle Φ_1 (the angle between the $\text{S}_2-\text{M}-\text{S}_3$ and $\text{S}_4-\text{M}-\text{S}_5$ planes). From the results of early refinements it became clear that $r(\text{C}_6-\text{N}_8)$ and $r(\text{C}_{10}-\text{N}_8)$ were highly correlated. Accordingly the average of the two values and the difference between them were refined. When the "best" values was obtained for the difference, it was fixed in the final least-squares refinement while the remaining parameters were refined. The resulting data are given in Table I.

Root-mean-square vibrational amplitudes (l), perpendicular amplitude corrections (k), and centrifugal distortion constants (δr) were calculated by using the earlier force field published for bis(dimethyldithiocarbamato)nickel(II).¹⁴

A model was tested in which the methyl groups were allowed to rotate. The resulting refinements showed no improvement over those in which the methyl groups were held in either a fixed eclipsed or a staggered position. For the copper compound a model was tested that allowed for the CNC_2 fragment of a S_2CNMe_2 group to come out of the appropriate CuS_2 plane by the angle Ψ_2 . The model was designed so that the two S_2CNMe_2 groups would be allowed to undergo a symmetrical deviation, giving rise to a "stepped" molecule. Such "stepped" species have been postulated to be formed by $[\text{Cu}(\text{MeCOCHCOMe})_2]$.¹⁵ However, inclusion of this extra variable did not improve the fit between theoretical and experimental data, so the extra variable was discounted.

Refinements of the structure were carried out by the least-squares procedure¹⁶ by adjusting one theoretical curve to fit the two average experimental intensity curves (one from each of the two nozzle-to-plate distances) with use of a unit weight matrix. The average curves and the final theoretical curve, together with the difference curves, are depicted in parts a and b of Figure 2 for the copper and zinc compounds, respectively. The correlation matrices are shown in parts a and b of Table II for the copper and zinc compounds, respectively. The radial distribution (RD) curves (see Figure 3) were calculated in the usual manner

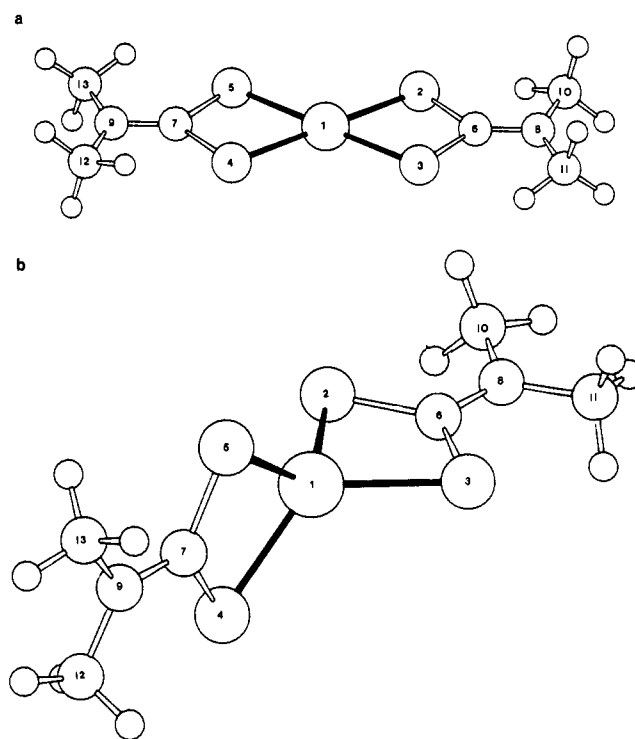


Figure 1. Molecules (a) $[\text{Cu}(\text{S}_2\text{CNMe}_2)_2]$ and (b) $[\text{Zn}(\text{S}_2\text{CNMe}_2)_2]$ with the atom-numbering schemes. The atom numbering is as follows: 1 = Cu (a), Zn (b); 2-5 = S; 6, 7, 10-13 = C; 8, 9 = N.

by Fourier transformation of the $s[I_m(s)]$ values after multiplication by $(Z_M Z_S / f_M f_S) \exp(-0.0025s^2)$ ($\text{M} = \text{Cu}, \text{Zn}$).

Results and Discussion

The results of our structural investigation of $[\text{Cu}(\text{S}_2\text{CNMe}_2)_2]$ and $[\text{Zn}(\text{S}_2\text{CNMe}_2)_2]$ by gas-phase electron diffraction reveal the influence of the d^9 configuration and the associated crystal field stabilization energy (CFSE) of the copper center upon the stereochemistry of the coordination sphere of the metal center. The two molecules are depicted in parts a and b of Figure 1 for $[\text{Cu}(\text{S}_2\text{CNMe}_2)_2]$ and $[\text{Zn}(\text{S}_2\text{CNMe}_2)_2]$, respectively, from which it is apparent that in the zinc compound the ZnS_4 fragment has D_{2d} symmetry with the ZnS_2S_3 plane being at right angles to the ZnS_4S_5 plane. In contrast, the CuS_4 fragment in the copper compound is planar, having D_{2h} symmetry. The major difference

- (12) *International Tables for X-ray Crystallography*; Kynoch: Birmingham, U.K., 1974.
 (13) Sellers, H. L.; Schafer, L.; Bonham, R. A. *J. Mol. Struct.* **1978**, *49*, 125.
 (14) Jensen, K. A.; Mynster Dahl, B.; Nielsen, P. H.; Borch, G. *Acta Chem. Scand.* **1972**, *26*, 2241.
 (15) Shibata, S.; Sasase, T.; Ohta, M. *J. Mol. Struct.* **1983**, *96*, 347.
 (16) Hedberg, K.; Iwasaki, M. *Acta Crystallogr.* **1964**, *17*, 529.

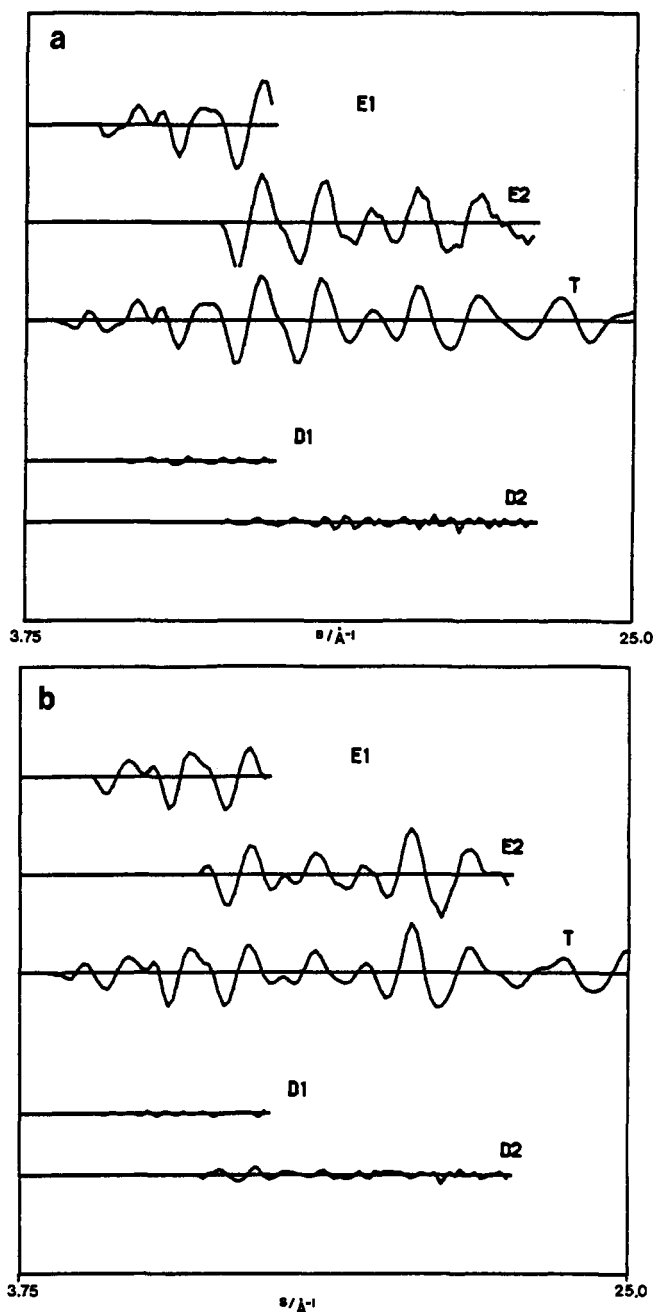


Figure 2. Intensity curves $s[I_m(s)]$ for (a) $[\text{Cu}(\text{S}_2\text{CNMe}_2)_2]$ and (b) $[\text{Zn}(\text{S}_2\text{CNMe}_2)_2]$. Experimental curves (E1 and E2) are averages of all plates for the two camera distances. The theoretical curves (T) were calculated from the structural parameters shown in Table I. The difference curves (D1 and D2) result from subtracting the relevant part of the theoretical curve from the experimental curves.

in nonbonded distances between the zinc and copper compounds becomes apparent by comparing the nonbonded S...S distances (see Table I), of which there are three types in each molecule. As the $\angle\text{S}-\text{M}-\text{S}$ angles are equivalent in both structures, the difference in $r(\text{S}_2\cdots\text{S}_3)$ values is purely dependent upon the difference in $r(\text{M}-\text{S})$ ($\text{M} = \text{Cu}$, 2.284 (9) Å; $\text{M} = \text{Zn}$, 2.348 (8) Å), which in turn is within experimental error equal to the difference between the single-bond covalent radii for the two metals (0.08 Å). More revealing is an examination of $r(\text{S}_2\cdots\text{S}_3)$ ($\text{M} = \text{Cu}$, 3.539 (16) Å; $\text{M} = \text{Zn}$, 4.184 (13) Å, where the former distance is shorter than twice the van der Waals radius for sulfur (3.70 Å). The remaining S...S distance ($r(\text{S}_2\cdots\text{S}_4)$) is greater than twice the van der Waals radius for sulfur in both compounds ($\text{M} = \text{Cu}$, 4.575 (13) Å; $\text{M} = \text{Zn}$, 4.181 (13) Å). Thus, to attain a planar CuS_4 fragment the steric repulsion arising from the generation of two S...S distances of 3.539 (16) Å has to be overcome. One source of the necessary energy open to the copper(II)

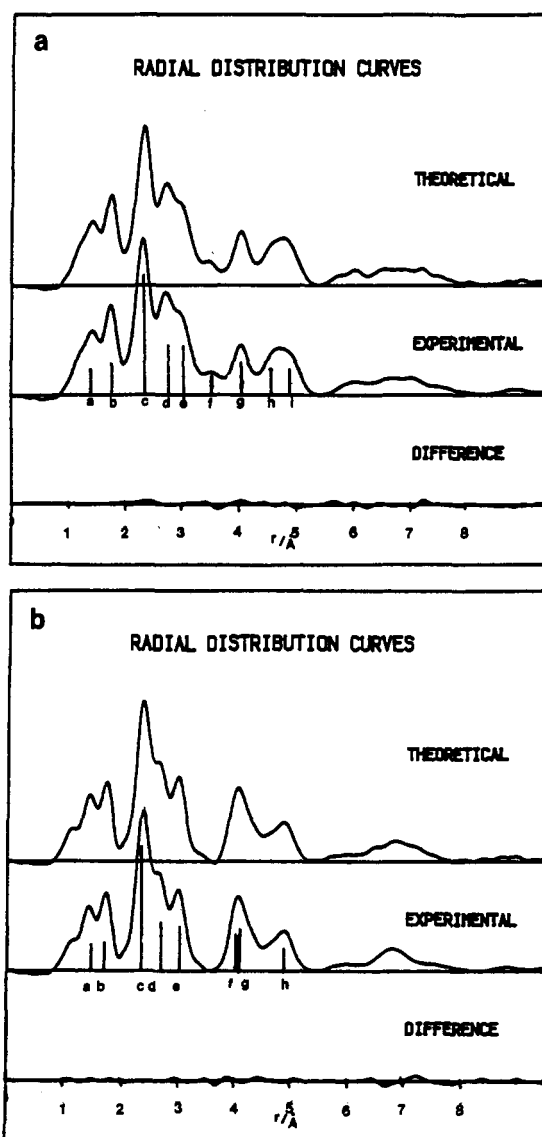


Figure 3. Radial distribution curves (a) for $[\text{Cu}(\text{S}_2\text{CNMe}_2)_2]$ and (b) $[\text{Zn}(\text{S}_2\text{CNMe}_2)_2]$ showing experimental, theoretical, and differences curves. The curves were calculated from the curves in Figure 2 after multiplying by $(Z_M Z_S / f_M f_X) \exp(-0.0025s^2)$ ($\text{M} = \text{Cu}, \text{N}$) and using theoretical data for the unobserved area $s < 3.75 \text{ \AA}^{-1}$. For such complicated molecules most of the peaks in the radial distribution curves are formed by contributions from one or more interactions. The positions of the major peaks are as follows: (a) a = C6-N8 and C10-N8, b = C6-S2, c = Cu-S2, d = S2...N8 and Cu...C6, e = S2...S3 and C10...S2, f = S3...S4, g = Cu...N9, h = S3...S5, i = Cu...C10; (b) a = C6-N8 and C10-N8, b = C6-S2, c = Zn-S2, d = S2...N8 and Zn...C6, e = S2...S3 and C10...S2, f = Zn...N9, g = S3...S5, h = Zn...C10.

compound but not the zinc(II) is of course crystal field stabilization energy (CFSE). The CuS_4 group could be expected to adopt either an approximately square planar or tetrahedral geometry. From simple crystal field theory the CFSE values (in terms of $Dq(\text{oct})$) for the two stereochemistries are $-12.28Dq(\text{oct})$ and $-1.78Dq(\text{oct})$ for square-planar and tetrahedral geometries, respectively.¹⁷ A value for $Dq(\text{oct})$ for Cu(II) in the pseudooctahedral dithiocarbamates is difficult to obtain because of the occurrence of charge-transfer bands in close proximity to the d-d bands. However, a value of 1800 cm^{-1} has been assigned to $Dq(\text{oct})$ for the square-planar nickel compound $[\text{Ni}(\text{S}_2\text{CNMe}_2)_2]$.¹⁸ With use of the Ni(II) values for $Dq(\text{oct})$ the difference in CFSE between square planar and tetrahedral can be calculated, and it is approximately 225 kJ mol^{-1} in favor of the square-planar

(17) Dunn, T. M.; McClure, D. S.; Pearson, R. G. *Some Aspects of Crystal Field Theory*; Harper and Row: New York, 1965.

(18) Fackler, J. P., Jr.; Coucouvanis, D. *J. Am. Chem. Soc.* **1966**, *88*, 3913.

Table II. Correlation Matrices ($\times 100$) for the Parameters in $[\text{Cu}(\text{S}_2\text{CNMe}_2)_2]$ and $[\text{Zn}(\text{S}_2\text{CNMe}_2)_2]$

(a) $[\text{Cu}(\text{S}_2\text{CNMe}_2)_2]$																
param	σ_{LS}^a	r_1	r_2	r_3	r_4	\angle_5	\angle_6	\angle_7	l_8	l_9	l_{10}	l_{11}	l_{12}	l_{13}	l_{14}	l_{15}
$r(\text{Cu-S})$	0.0021	100	10	-7	-16	-14	29	6	-2	6	34	37	55	-62	-17	10
$r(\text{C-S})$	0.0025		100	-6	-16	62	58	5	33	60	12	7	33	-29	-33	0
$r(\text{C-N})$	0.0044			100	26	53	-18	-24	-1	1	5	-2	20	-17	-29	13
$r(\text{C-H})$	0.0152				100	31	-52	-6	-9	-6	9	-11	-12	10	-1	5
$\angle\text{S-Cu-S}^b$	0.23					100	31	21	19	40	19	11	40	-23	-25	13
$\angle\text{N-C-H}$	2.15						100	9	14	29	48	41	46	-32	-21	13
$\angle\text{C-N-C}^b$	0.42							100	-2	3	12	17	-3	22	23	5
$l(\text{C-H})$	0.015								100	56	-13	-6	4	-4	-9	-2
$l(\text{C-N})$	0.011									100	-10	-2	17	-18	-20	-5
$l(\text{C-S})$	0.006										100	68	62	-41	-7	37
$l(\text{Cu-S})$	0.003											100	60	-46	-14	43
$l(\text{N}\cdots\text{S})$	0.008												100	-80	-26	29
$l(\text{Cu}\cdots\text{C})$	0.035													100	50	-23
$l(\text{S}\cdots\text{S})$	0.005														100	-19
$l(\text{Cu}\cdots\text{N})$	0.014															100

(b) $[\text{Zn}(\text{S}_2\text{CNMe}_2)_2]$																
param	σ_{LS}^a	r_1	r_2	r_3	r_4	\angle_5	\angle_6	\angle_7	l_8	l_9	l_{10}	l_{11}	l_{12}	l_{13}	l_{14}	
$r(\text{Zn-S})$	0.0021	100	13	-10	-7	-31	56	-15	-9	0	-21	9	-21	-15	-34	
$r(\text{C-S})$	0.0025		100	-22	-29	44	34	-22	1	31	4	10	-1	-14	1	
$r(\text{C-N})$	0.0043			100	48	48	-37	-50	4	2	14	-34	22	42	-14	
$r(\text{C-H})$	0.0108				100	12	-33	-13	-3	-12	10	-21	9	23	-5	
$\angle\text{S-Zn-S}^c$	0.20					100	-9	-42	2	21	15	-23	7	28	5	
$\angle\text{N-C-H}$	2.63						100	0	-10	12	-51	50	-56	-59	-31	
$\angle\text{C-N-C}^c$	0.40							100	-3	-8	-4	9	-10	-12	2	
$l(\text{C-H})$	0.012								100	12	16	-10	17	11	12	
$l(\text{C-N})$	0.015									100	18	6	1	-9	2	
$l(\text{Zn-S})$	0.004										100	-76	65	77	38	
$l(\text{N}\cdots\text{S})$	0.051											100	-60	-93	-25	
$l(\text{S}\cdots\text{S})$	0.007												100	62	49	
$l(\text{Zn}\cdots\text{C})$	0.045													100	24	
$l(\text{Zn}\cdots\text{N})$	0.038														100	

^aStandard deviations taken from the least-squares refinement. Distances (r) and amplitudes (l) in angstroms and angles in degrees. ^b $\angle\text{S-Cu-S}$ is $\angle\text{S}_3\text{-Cu-S}_2$; $\angle\text{C-N-C}$ is $\angle\text{C}_6\text{-N}_8\text{-C}_{10}$. ^c $\angle\text{S-Zn-S}$ is $\angle\text{S}_3\text{-Zn-S}_2$; $\angle\text{C-N-C}$ is $\angle\text{C}_6\text{-N}_8\text{-C}_{10}$.

configuration. The importance of such a value can be judged by considering the bond dissociation enthalpies of Br_2 , Cl_2 , and C-I , which are 193, 242, and 238 kJ mol^{-1} , respectively. Thus, $[\text{Cu}(\text{S}_2\text{CNMe}_2)_2]$ is to be expected to adopt a D_{2h} configuration in the gas phase as the energy savings from CFSE is more than enough to form two $r(\text{S}_2\cdots\text{S}_2)$ interactions of 3.539 (16) Å.

As stated in the Introduction, the solid-state structures of both $[\text{Zn}(\text{S}_2\text{CNMe}_2)_2]^4$ and $[\text{Cu}(\text{S}_2\text{CNMe}_2)_2]^5$ have been determined. Although the coordination sphere of the zinc atoms in both the gas phase and solid phase is pseudotetrahedral, the mode of ligand bonding differs. In the solid state each zinc atom is bound to one chelating (Zn-S distances 2.333 (6) and 2.429 (6) Å) and two bridging $[\text{S}_2\text{CNMe}_2]$ groups (Zn-S distances 2.373 (6) and 2.312 (6) Å). The formation of bridging rather than chelating $[\text{S}_2\text{CNMe}_2]$ groups reduces the strain in the ligand that arises from the presence of Zn-S-C-S rings. In contrast in the solid state two chelating $[\text{S}_2\text{CNMe}_2]$ groups are found in the copper compound (Cu-S distances 2.302 (2) and 2.319 (2) Å). However, in addition there is an extra type of interaction with one sulfur atom from each $[\text{S}_2\text{CNMe}_2]$ group forming a long-range interaction with other copper atoms on adjacent molecules (Cu-S distance 3.159 (3) Å), thus giving rise to six-coordinate copper

atoms. The Cu-S and Zn-S distances in the gas-phase determinations (Cu-S , 2.284 (9) Å; Zn-S , 2.348 (8) Å) are in accord with the data from the solid-state studies. Similarly all the bond angles and distances in the chelating $[\text{S}_2\text{CNMe}_2]$ groups found in the present studies agree with those found in the solid state. It should be noted that the data obtained in this electron diffraction study, even for correlated distances, are of a higher accuracy than those obtained by X-ray methods.

Conclusions

The study has further demonstrated that electron diffraction is a good method for studying the coordination sphere of metals in their complexes free from the influences of the crystal lattice and, thus, the true impact of crystal field stabilization energy upon the geometry of a metal's coordination sphere can be demonstrated.

Acknowledgment. We thank Snefrid Gundersen and Hans Volden of the University of Oslo for their technical help, the SERC for the financial support of C.J.H., and NATO for the award of the travel grant (Grant No. 117/82). Special thanks are due to Alan Adams of the University of Reading for his help in building the electron diffraction apparatus.

Registry No. $\text{Cu}(\text{S}_2\text{CNMe}_2)_2$, 137-29-1; $\text{Zn}(\text{S}_2\text{CNMe}_2)_2$, 137-30-4.